Colloid Polym Sci 275:1121–1135 (1997)

ORIGINAL CONTRIBUTION

H. Janeschitz-Kriegl

Conditions of nucleation in crystallizable polymers: reconnaissance of positions – a critical evaluation

Received: 3 June 1997
Accepted: 19 August 1997

Dedicated to Prof. W.J. Beek, Delft

H. Janeschitz-Kriegl (✉)
Institute of Chemistry
Linz University
A-4040, Austria

Abstract In view of the enormous difficulties in obtaining reliable experimental data for the purpose of structure simulation with the aid of computer programs (presently being so popular), every classifying endeavor must be considered of great importance. One of the goals of such an endeavor is the demarcation of characteristic temperature ranges. With the aid of thermodynamic considerations an estimate of the restricted temperature range of metastable undercooling, in which the classical theory of homogeneous nucleation, as developed for polymer solutions, is valid also for polymer melts ("thermal nucleation") can be given. This consideration includes a discussion of the course of the relevant interface tensions along the co-existence lines of the P–T diagram. The so-called spinodal crystallization mode (see [1–3]) is found at lower temperatures and seems to be quite common in polymer crystallization. In this connection the so-called athermal nucleation can be identified with a specific process. However, the present author is not in favor of the term "spinodal mode". This is explained by a comparison with the meaning of spinodal decomposition into two phases in the ordinary gas–liquid phase transition, which always occurs at the lower bound of the metastable undercooling. Remarkably, spinodal decomposition cannot be defined in the same way for the liquid–solid transition. Anyway, the author tries hard to induce unorthodox trains of thought in the hope to revive the discussion of a difficult matter, which has almost gone to sleep, before a satisfying settlement has been reached.

Key words Metastable undercooling – spinodal mode – thermal history – interface tensions – morphology – backbone mobility

General introduction

As is well-known, for the description of the kinetics of primary homogeneous "sporadic" nucleation, also known under the name "thermal" nucleation, the following equation, as given first by Becker [4] has frequently been used:

$$v = K \exp\left(-\frac{E_a}{kT}\right) \exp\left(-\frac{\Delta g_m}{kT}\right), \quad (1)$$

where v is the frequency of the formation of primary nuclei per unit of volume, $K(=kT/h)$ is practically a constant, E_a is an activation energy and Δg_m is a kinetic barrier related to the fact that the creation of a new phase is hampered by the formation of an interface (kT has the usual meaning). If this v is plotted against temperature, one obtains a bell-shaped curve, which has, if the parameters are chosen adequately, a maximum halfway between the glass-transition temperature T_g and the melting point T_m. At T_m

and near T_g it should go to zero. This Eq. (1) is the basis of the classical theory of primary homogeneous sporadic nucleation. The occurrence of a frequency ν is characteristic for this type of nucleation. Because of the fact that in many cases heterogeneous nucleation prevails, as is caused by the presence of dust particles or other impurities or, purposely, by the addition of nucleation agents, homogeneous primary nucleation has not received too much interest. In the present paper, however, homogeneous primary nucleation is considered as the basic process for processes occurring in connection with steep temperature gradients, complicated temperature histories and flow. In this connection it will be emphasized that, besides the said sporadic nucleation, there is a second type of homogeneous nucleation, which seems specific for polymers. It has been called "athermal" nucleation [5]. For its appreciation, however, the lower bound of the temperature range, i.e. the metastable range of undercooling, in which the sporadic nucelation prevails, must first be found. How this goal can be accomplished, will be shown in the present paper.

According to Becker and Döring [6] in thermal nucleation the kinetic barrier reads for a nucleus of spherical shape with radius r:

$$\Delta g = \frac{4\pi}{3} r^3 \frac{\rho}{M} \Delta\mu + 4\pi r^2 \sigma \,, \tag{2}$$

where $\Delta\mu$ is the difference between the chemical potentials (i.e. per mol of the substance!) in the new and in the old phases (being negative with undercooling), ρ is the density of the new phase, M is the molar mass and σ is the interfacial tension. Tacitly, the new phase is considered as a continuum containing a sufficient number of molecules. This assumption, of course, is not always realistic.

The first derivative of Δg with respect to r is zero at $r = 0$ and at a critical value

$$r_m = 2\sigma M / |\Delta\mu| \rho \,, \tag{3}$$

where Δg shows a maximum

$$\Delta g_m = \frac{16\pi}{3} \frac{\sigma^3 M^2}{(\Delta\mu)^2 \rho^2} \,. \tag{4}$$

Only if in the melt a nucleus with a radius larger than r_m is formed spontaneously, it can grow because of the fact that according to Eq. (2) Δg decreases on the "right" side of the maximum with further increasing radius r. Equation (1) only works if

$$\Delta g_m \geq kT \,,$$

which means that the events for the formation of a critical nucleus must be rare ("sporadic"). Otherwise the second term of Eq. (1), a term of the Boltzmann type, becomes insufficient for a correct description. (In fact, it only gives the probability for the occurrence of a cluster of suitable size.) As Ziabicki and Alfonso [7] have recently shown, one can give a correct description of the pertinent "growth diffusion" against the "left" slope of the barrier of Eq. (2) in terms of a suitable Fokker–Planck equation with an "absorbing wall" as the adequate boundary condition. Unfortunately, the authors were not able to give the resulting flux over the barrier (into the "absorbing wall") in terms of measurable parameters.

For $\Delta\mu$ thermodynamics provides a very useful first approximation in terms of the undercooling $\Delta T = (T_{tr} - T)$, where T_{tr} is the equilibrium temperature of the transition. This approximation reads

$$\Delta\mu = -\frac{\Delta H_{tr}}{T_{tr}} \Delta T \,, \tag{5}$$

where ΔH_{tr} is the molar latent heat of the transformation. (See for the derivation of this equation the second of Eq. (7) below with the well-known equilibrium condition $\Delta G_{tr} = 0 = \Delta H_{tr} - T_{tr} \Delta S_{tr}$.) Using this approximation in the second exponential factor of Eq. (1) one obtains a flux, which apparently does not sufficiently increase with decreasing temperature. In this connection one should look up Binsbergen's [8] early homophonous comments, which are based on a computer simulation.

One of the difficulties with Eqs. (3) and (4) is that our knowledge of σ is rather poor. Only one thing is sure: in the equilibrium situation σ does not vanish, in contrast to $\Delta\mu$. As a consequence, a reasonable approximation will be for not too large values of ΔT:

$$\Delta g_m = \frac{16\pi}{3} \frac{\sigma^3 M^2 T_{tr}^2}{\rho^2 \Delta H_{tr}^2} \frac{1}{(\Delta T)^2} \,, \tag{6}$$

where the total factor of $(1/\Delta T)^2$ is a thermodynamic equilibrium property at $T = T_{tr}$.

In that which follows two routes will be pursued: For the gas–liquid transition we use the well-known occurrence of a spinodal transition for guessing the range of metastable undercooling. This guess has the advantage of being independent of any nucleation theory. Unfortunately, a spinodal transition does not exist for the liquid–solid transition. (The author is extremely grateful to his colleague in theoretical physics at Linz university for pointing him to this fact. See the acknowledgements.) So, one has to return to the primitive barrier concept for a judgement of this latter transition. Possible barriers for an ordinary liquid–solid transition can be derived from equilibrium values of the interface tensions σ_{gl} and σ_{ls}, as obtained at the triple point. Finally these experiences are used for polymer crystallization, where the first exponential term of Eq. (1) (an Arrhenius term or a nearly equivalent Vogel–Fulcher term) becomes predominant. Also lamellar growth has to be discussed in this connection. The reason for this necessity is of particular interest: It will appear that already existing but dormant athermal nucleation sites of varying quality can become effective only if their conditions of "sprouting" are fulfilled. Here one will find the explanation for the fact that the number of effective athermal nucleation sites per unit volume grows tremendously (by many decades) with increasing undercooling. (See [9]) This happens in a temperature range far below the lower bound of thermal nucleation.

As far as possible, the early criticism on the concept of a surface tension barrier, as put forward by Binsbergen [10] for thermal nucleation, should not completely be ignored. In Binsbergen's theory the fact is taken into account that, in general, the number of molecules per cluster is insufficient for a treatment of the cluster as a thermodynamic system. However, the intended overview will only be possible with the aid of the simpler classical approach. Anyway, the necessary care will be bestowed for any conclusion to be drawn.

PART I. GENERAL CONSIDERATIONS

Undercooling with gas–liquid phase transition

The gas–liquid transition has been chosen first because of its simple physics, when compared with the liquid–solid transition. For the gas–liquid transition one is tempted to propose a description in terms of an isobaric $T(S)$-diagram instead of the more common isothermal $P(V)$-diagram. (T – abs. temperature, S – molar entropy, P – pressure, V – molar volume.) The latter diagram is familiar from the famous Van Der Waals equation for the gas–liquid phase transition. However, it is also known, that with this equation a description of undercooling or superheating is quite troublesome (in terms of the unwieldy isotherms as given by this equation). So, an isobaric diagram would seem of great value. As is well known, variables like P and V are interchangeable in the pertinent Maxwell relations. The same holds for T and S, where in both cases the first variable is intensive, whereas the second one is extensive. The meant Maxwell relations are:

$$\left(\frac{\partial H}{\partial S}\right)_P = T, \quad \left(\frac{\partial G}{\partial T}\right)_P = -S;$$

$$\left(\frac{\partial F}{\partial V}\right)_T = -P, \quad \left(\frac{\partial G}{\partial P}\right)_T = V, \qquad (7)$$

where H is the molar enthalpy, F is Helmholtz's molar free energy and G is the molar free enthalpy, i.e. Gibbs' molar free energy.

In Fig. 1 the desired isobaric diagram is shown schematically. Somewhat unusually S is used as the independent variable. However, the present form of the figure is chosen in analogy to Van Der Waals' well-known diagram. The equilibrium lines for T vs. S are drawn as solid thick lines for three pressures, the highest one being the critical pressure. The binodal curve is drawn through the end-points of the horizontal connodes connecting the points for the entropies of the co-existing gaseous and liquid phases. ($T(S)$-diagrams are found in a well-established textbook on thermodynamics [11].) Meandering curves are now inserted in our diagram for the two pressures below the critical one. These curves are meaningful like those known from Van Der Waals. In fact, a liquid can be superheated and a gas can be undercooled. These processes correspond to the branches of the meandering curves with positive slopes. The central part with negative slope indicates the region of instability. Because $H(S)$ is a function of state, the path of integration between the end-points of the connodes should be of no influence (see Eq. (7)). This means that the areas between a connode and the upper and lower branches of the pertinent meandering curve must be equal. This fact furnishes a well-come limitation for the degree of undercooling (or superheating), at the same time avoiding the introduction of an a priori unknown value of an interface tension. Somehow, this

Fig. 1 Isobaric T–S diagram for the gas–liquid transition (schematic). The metastable ranges of undercooling and superheating are clearly recognizable as the areas between the binodal and the (dashed) spinodal lines

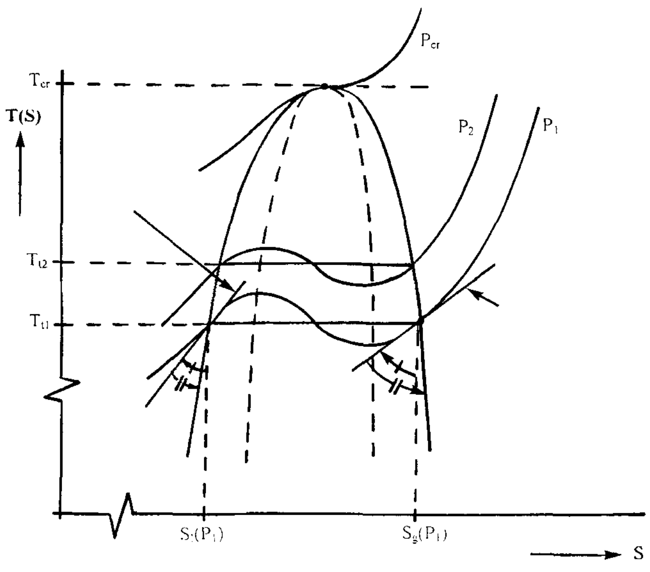

interface tension must be an effective quantity, merely expressing the fact that the clusters (or the unfolding voids) still do not consist of sufficiently dense (or dilated) matter.

For the construction of the binodal curve in Fig. 1 the following Taylor series is of importance:

$$S(T_2,P_2) = S(T_1,P_1) + (T_2 - T_1)\frac{C_{P_1}}{T_1} - (P_2 - P_1)\left(\frac{\partial V}{\partial T}\right)_{P_1} . \tag{8}$$

As a further parameter this equation contains the specific molar heat C_{p1} of the phase corresponding to the chosen end-point of the connode. As is well known, the coefficients of this equation can be derived from the following relations:

$$\left(\frac{\partial S}{\partial T}\right)_P = \frac{C_P}{T}; \quad \left(\frac{\partial S}{\partial P}\right)_T = -\left(\frac{\partial V}{\partial T}\right)_P . \tag{9}$$

It should also be observed that P and T are interdependent through an equation of state like the one given by Van Der Waals.

In Fig. 1 tangents are drawn at the end-points of the connode for pressure P_1. If now vertical (dashed) lines are drawn through these end-points, pointing to the corresponding entropy values at the S-axis, one can understand the deviations from these entropies with the aid of the curved arrows inserted in the graph. The arrow with one mark stands for the second term on the right side of Eq. (8), whereas the arrow with two marks stands for the third term of Eq. (8). In fact, the influence of thermal expansion is large for the gas, but small for the fluid. This explains, why at the side of the gas the binodal can have a negative slope, whereas the slope of the isobar remains positive also in the pseudo-equilibrium branch. In a well-known way the boundary of the region of instability is given by the spinodal lines going through the maxima and minima of the meandering curves. It goes without saying that no noticeable undercooling or superheating occurs at sufficiently low cooling or heating rates. At higher rates the access to the metastable regions is more easy, but it is only granted as long as the flux over the said barrier is low compared with the rates of attachment and detachment of molecules to temporary clusters in the undercooled gas or to incipient voids in the superheated fluid. It is obvious that these latter rates are still similar to those in the contiguous thermodynamically stable phases. Otherwise one ends up at the other side of the temperature range for metastable undercooling, viz at its lower bound. In the main part of the metastable range the only reason for the delay in the transition is given by the interfacial barrier. If this barrier approaches zero, as happens near the minima and the maxima of the meandering curves, the transition occurs with a speed comparable to that of the cluster formation, which becomes very large compared with the speed of spontaneous cluster decay. Here the clusters may be assumed to be dense enough. In the gas–liquid transition the mentioned speed will be high. From a linguistic point of view the term "spinodal" seems to express this fact.

For the case that the considerations are extended to more viscous systems, where the first exponential factor of Eq. (1) becomes of importance, the use of the ratio of the rates of attachment and detachment seems more convenient. This ratio is much less dependent on the viscosity of the system than the separate parameters. In the middle of the temperature range of metastable undercooling this ratio is still of the order of unity. However, at temperatures below the minimum of the meander of Fig. 1 its value increases rapidly. But this does not necessarily mean that the rate of attachment itself must increase. On the contrary, it very often will decrease. One should not forget in this connection that, with decreasing temperature, the viscosity of the system can increase even more rapidly than the said ratio.

One may also notice that with P–V and with T–S diagrams one has for the phase transitions:

$$P_{\mathrm{tr}} = P_{\mathrm{tr}}(T) \quad \text{and} \quad T_{\mathrm{tr}} = T_{\mathrm{tr}}(P) , \tag{10}$$

respectively. An alternative presentation in terms of an integrated version (see again Eq. (7)) can also be provided. This is shown in Fig. 2, where H is given as a function of S (ΔH_{tr} and ΔS_{tr} represent themselves in this graph directly). A rough description of the heat balance seems of importance. If during undercooling the isobar starts to deviate to the left (see Fig. 1) from the extrapolated isobar of the gas, the evolution of latent heat sets in. For this simplified description the deviations of T from T_{tr} can be disregarded. Because of $\Delta H_{\mathrm{tr}} = T_{\mathrm{tr}} \Delta S_{\mathrm{tr}}$ one can be quite sure that for a cooling process the latent heat is evolved for a great deal in the region of instability between the minimum and the maximum of the isobar. In fact, during a cooling cycle roughly one quarter of this heat is needed for bringing back the temperature of the undercooled sample to T_{tr}, another quarter is needed for a subsequent heating of the sample to the maximum temperature of superheating. The remaining half of the heat is lost to the surroundings of the sample by direct heat transfer as in the regions of metastable cooling.

A reasonable estimate of the limit of metastable undercooling can now easily be given for the gas–liquid transition. It reads

$$\int_{T_{\mathrm{u}}}^{T_{\mathrm{b}}} \frac{C_{\mathrm{p,g}}}{T}\,\mathrm{d}T \approx \frac{1}{3}\Delta S_{\mathrm{b}} , \tag{11}$$

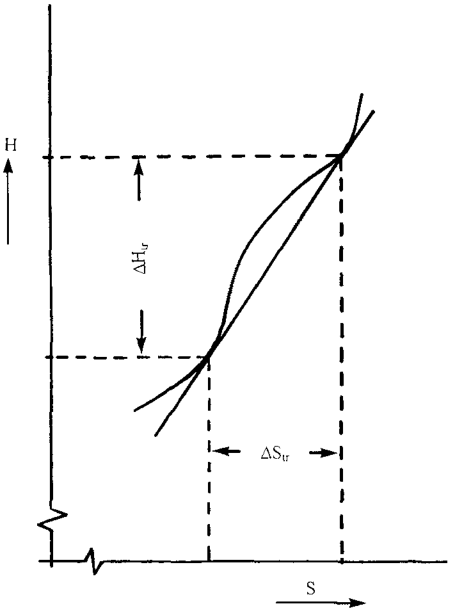

Fig. 2 Schematic diagram showing the integrated version of Fig. 1 for one pressure. From this figure one can learn that isobars, as shown in Fig. 1, cannot show too exotic shapes even with the liquid–solid transition

where T_u is the lower temperature limit of undercooling, T_b is the equilibrium boiling point, $C_{p,g}(T)$ is the molar heat of the gas as a function of temperature along the extrapolated isobar and ΔS_b is the molar entropy of vaporization (i.e. 88 J/mol K for "normal" fluids according to the rule of Trouton). A factor 1/3 is chosen for the right side of Eq. (11) instead of a factor 1/4, as suggested by the picture. This higher factor is chosen because of the deviation of the meander from the accurate skew symmetry, as caused by the fact that always $C_{p,g} > C_{p,l}$.

One may also notice that the prolonged isobar does not show the minimum of the meander. So, the value of the undercooling $T_b - T_u$, as obtained from Eq. (11), is certainly an overestimate. Since $T_b/C_{p,g}(T_b)$ is the tangent of the curve $T(S)$ at the point (T_b, S_g), one can obtain a more practical but even more pronounced overestimate with the aid of the equation:

$$(C_{p,g}/T_b)(T_b - T_u) = (1/3)\Delta S_b \,. \tag{12}$$

It will be seen below that this – certainly much too high – value of $T_b - T_u$ will suit our purpose. With the aid of the data for nonadecane, as contained in Table 1 – nonadecane is judged a suitable model fluid with polymer like behaviour – one calculates a value of 94 J/mol K for ΔS_b ($= H_b/T_b$). This value is rather close to the value demanded by the rule of Trouton. With the aid of Eq. (12) one obtains $T_b - T_u \cong 25$ K. With this undercooling and using the obvious condition $\Delta g_m = kT_b$ one obtains from Eq. (6) an estimate of the apparent interface tension at the boiling point of nonadecane of 2.3 mN/m. This value will be used later for the purpose of comparison.

As Eder [12] has shown recently, the $T(S)$-diagram of the Van Der Waals model can readily be calculated. The obtained meanders are rather smooth like those in Fig. 1. But this would mean that $T_b - T_u$ is overestimated by Eq. (12) by a factor of about two. The corresponding value of the surface tension would then be about one half of the given value. However, as already indicated, factors of one half or two are not relevant for our reasoning, where much higher factors are at stake.

Interfacial tension at the co-existence lines of the *P–T* diagram

In discussions with his colleague in theoretical physics (see the acknowledgements) the attention of the author was drawn to the fact that a meandering curve cannot be constructed for the liquid–solid transition. However, the author conjectured that in the temperature range of metastable undercooling (more or less ordered solid) clusters will appear first, similar to liquid clusters in the gas–liquid transition. But, in contrast, no voids can occur in the superheated crystal! Also, the pertinent kinetic barriers of the gas–liquid and the liquid–solid transitions should not be very different, at least for low molar mass compounds (see later). In fact, one may argue that a cluster,

Table 1 Required physical data of nonadecane*)

	Temperatures [°C]	[K]	Pressure P_{cr} [bar]	Densities ρ_l [kg/m^3]	ρ_g [kg/m^3]	Latent heat $\Delta H_b/M$ [J/kg]	Heat capacity $C_{p,g}/M$ [J/kg K]
	20		1	788			
T_m	32.1	305.3	1	780			
T_b	330	603.2	1	540	5.4	2.11×10^5	2.85×10^3
T_{cr}	487	760.2	12				

*) From VDI-Wärmeatlas, 1977.

as it is primarily formed in the undercooled liquid, behaves more like a fluid particle and still does not know that there will be extra conditions for the final solidification. For a more quantitative estimate, however, one has to have recourse to the variation of the interface tension, as occurring during a journey along the co-existence lines. The involvement of the co-existence lines is dictated by the fact that the (total) factor of $(1/\Delta T)^2$ in Eq. (6) is an equilibrium property.

A differential equation for the dependence of the interfacial tension on temperature and pressure, as characteristic for the co-existence lines, can be derived from the pertinent Gibbs–Duhem equation. This equation reads

$$\mathrm{d}\sigma = -\varepsilon(S^{\mathrm{v},\sigma} - S^{\mathrm{v}})\,\mathrm{d}T - \varepsilon(N^{\mathrm{v},\sigma} - N^{\mathrm{v}})\,\mathrm{d}\mu\,, \qquad (13)$$

where, in principle, ε is the arbitrarily chosen thickness of the interfacial layer between the two phases, S^{v} and N^{v} are the entropy and the number of molecules per unit of volume in the denser homogeneous phase, and $S^{\mathrm{v},\sigma}$ and $N^{\mathrm{v},\sigma}$ are the respective (average) quantities per unit of volume in the interfacial layer. As is well known, the thickness of the interfacial layer must be chosen large enough in order to avoid inhomogeneities outside this layer. Any arbitrary change in the value of ε causes adequate variations in $S^{\mathrm{v},\sigma}$ and $N^{\mathrm{v},\sigma}$, so that the total "surplus", as projected mentally into the interface, remains constant. This remark is necessary in view of the fact that the pressure differential $\mathrm{d}P$ does not show up explicitly in Eq. (13). In fact, according to the well-known reasoning by Gibbs volume elements εA of equal size, where A is the total area of the interface, are cut out of the denser homogeneous phase and of the said layer and are compared with each other. The size of these volume elements is chosen arbitrarily within the above-mentioned limits. So, it does not depend on the applied pressure.

If one assumes now for simplicity that the boundaries of the interfacial layer are sharp and that the density within this layer changes linearly from that of the more condensed phase to that of the more dilated phase, one obtains a distinct value

$$V^{\sigma} = \varepsilon A \qquad (14)$$

for the volume of the interfacial layer. For this special layer the average density becomes

$$\rho^{\sigma} = (\rho_{\mathrm{l}} + \rho_{\mathrm{g}})/2\,. \qquad (15)$$

where the subscripts "l" and "g" (for "liquid" and "gas") are chosen to be representative for the more condensed and the more dilated phase. For a liquid–solid transition "l" is simply replaced by "s" and "g" by "l". It should be stated clearly at this point that ε is now just a parameter characteristic for the course, which the density takes within the interfacial layer. Of course, it can slightly change along the coexistence lines and will be commensurable with the intermolecular distances.

With these assumptions one has

$$S^{\mathrm{v},\sigma} - S_{\mathrm{l}}^{\mathrm{v}} = \frac{1}{M}\left[S^{*,\sigma}\frac{\rho_{\mathrm{l}} + \rho_{\mathrm{g}}}{2} - S_{\mathrm{l}}^{*}\rho_{\mathrm{l}}\right], \qquad (16)$$

where in this section the terms for molar quantities are designated by an asterisk for the purpose of distinction from so many other symbols. A slight rearrangement gives

$$S^{\mathrm{v},\sigma} - S_{\mathrm{l}}^{\mathrm{v}} = \frac{1}{M}\left[(S^{*,\sigma} - S_{\mathrm{l}}^{*})\frac{\rho_{\mathrm{l}} + \rho_{\mathrm{g}}}{2} - S_{\mathrm{l}}^{*}\frac{\rho_{\mathrm{l}} - \rho_{\mathrm{g}}}{2}\right]. \qquad (17)$$

Because of the fact that an equilibrium situation for which the chemical potential is the same in both homogeneous phases as well as in the interfacial layer is considered, one has also for the matter in the interface:

$$\Delta G^{*,\sigma}(=\Delta\mu) = 0 = \Delta H^{*,\sigma} - T\,\Delta S^{*,\sigma}\,. \qquad (18)$$

With the use of Eq. (18) one finally arrives at

$$S^{\mathrm{v},\sigma} - S_{\mathrm{l}}^{\mathrm{v}} = \frac{1}{M}\left[\frac{\Delta H^{*,\sigma}}{T}\frac{\rho_{\mathrm{l}} + \rho_{\mathrm{g}}}{2} - S_{\mathrm{l}}^{*}\frac{\rho_{\mathrm{l}} - \rho_{\mathrm{g}}}{2}\right]. \qquad (19)$$

One also has

$$N^{\mathrm{v},\sigma} - N_{\mathrm{l}}^{\mathrm{v}} = -\frac{1}{M}(\rho_{\mathrm{l}} - \rho_{\mathrm{g}})\,. \qquad (20)$$

For the use in Eq. (13), however, we also need a relation for $\mathrm{d}\mu$. This relation is gained as follows:

$$\mathrm{d}\mu = \left(\frac{\partial\mu}{\partial P}\right)_T \mathrm{d}P + \left(\frac{\partial\mu}{\partial T}\right)_P \mathrm{d}T = V_{\mathrm{l}}^{*}\,\mathrm{d}P - S_{\mathrm{l}}^{*}\,\mathrm{d}T\,. \qquad (21)$$

For our purpose we can write Clapeyron's equation as follows:

$$\mathrm{d}P = \frac{\rho_{\mathrm{l}}\rho_{\mathrm{g}}}{M}\frac{S_{\mathrm{g}}^{*} - S_{\mathrm{l}}^{*}}{\rho_{\mathrm{l}} - \rho_{\mathrm{g}}}\,\mathrm{d}T\,. \qquad (22)$$

This equation describes the course of P as a function of T along the co-existence lines of the P–T diagram. Inserting this expression together with $V_{\mathrm{l}}^{*} = M/\rho_{\mathrm{l}}$ into Eq. (21) one obtains

$$\mathrm{d}\mu_{\mathrm{l}} = \frac{1}{\rho_{\mathrm{l}} - \rho_{\mathrm{g}}}\left[\rho_{\mathrm{g}}S_{\mathrm{g}}^{*} - \rho_{\mathrm{l}}S_{\mathrm{l}}^{*}\right]\mathrm{d}T\,. \qquad (23)$$

It is satisfactory that one arrives exactly at the same expression, if one starts in Eq. (21) with V_{g}^{*} and S_{g}^{*}. This, of course, means that

$$d\mu_l = d\mu_g \,, \tag{24}$$

as it should be because of $\Delta\mu = 0$. Using Eqs. (23), (21) and (19) in Eq. (13) one arrives at

$$d\sigma_{lg} = -\frac{\varepsilon}{2M}\frac{1}{T}\left[\Delta H^{*,\sigma}(\rho_l + \rho_g) - \rho_g \Delta H_b^*\right] dT \,, \tag{25}$$

where also the substitution $\Delta S_b^* = \Delta H_b^*/T$ is applied. The subscript "b" is omitted for T because of the tacit assumption of a journey along the co-existence line.

Finally one may argue that $\Delta H^{*,\sigma}$ must be proportional to ΔH_b. For simplicity we assume

$$\Delta H^{*,\sigma} \cong 1/2 \Delta H_b^* \,. \tag{26}$$

So, one arrives at

$$\frac{d\sigma_{lg}}{dT} = -\frac{\varepsilon}{4M}(\rho_l - \rho_g)\frac{\Delta H_b^*(T)}{T} \,. \tag{27}$$

In principle one can integrate this equation along the gas–liquid line, if at one temperature a measurement furnishes a starting value for the surface tension. The transition from the gas–liquid line to the liquid–solid line can be accomplished via the triple point, where the chemical potential is equal in all the three phases involved. This statement will be underpinned right away.

According to classical thermodynamics one has

$$\sigma = \left(\frac{\partial G_l}{\partial A}\right)_{P,T} = V_l\left(\frac{\partial G_l^v}{\partial A}\right)_{P,T} \,, \tag{28}$$

where G^v is the Gibbs free enthalpy per unit volume. For two homogeneous phases one has in equilibrium with $G^* \equiv \mu$:

$$G_l^v = \frac{\mu}{M}\rho_l \quad \text{and} \quad G_g^v = \frac{\mu}{M}\rho_g \,. \tag{29}$$

This means that, approximately, one has for the interfacial layer per unit area

$$g^\sigma = \varepsilon\frac{\mu}{M}\frac{\rho_l + \rho_g}{2} \,. \tag{30}$$

If a volume element εA (with $A = 1$) from the interior of the more condensed phase is compared with a volume element of equal size comprising the interface, one has

$$\sigma_{lg} = \Delta g^\sigma = g^\sigma - g_l = -\varepsilon\frac{\mu}{M}\frac{\rho_l - \rho_g}{2} \,. \tag{31}$$

This equation seems surprisingly simple. However, the value of μ is completely unknown, except for the fact that it is negative. This is the reason why we must have resource to the temperature T_3 at the triple point, where we at least know that μ is equal in all the three relevant phases, the crystalline, the liquid and the gaseous phase. So, we can at least compare the respective values of σ at this point.

With the aid of Eq. (31) and a similar one for the liquid–solid interface one obtains at the triple point

$$\frac{\sigma_{lg}}{\sigma_{sl}} = \frac{\varepsilon_{lg}}{\varepsilon_{sl}}\frac{\rho_l - \rho_g}{\rho_s - \rho_l} \cong \frac{\varepsilon_{lg}}{\varepsilon_{sl}}\frac{V_s}{V_l - V_s} \,. \tag{32}$$

With the aid of Eqs. (27) and (32) one can now construct the temperature dependence of the interface tensions for the equilibria along the co-existence lines. A direct integration, however, fails because of the lack of accurate data for the densities and for the latent heats as functions of the equilibrium temperatures. One only knows that in the gas–liquid phase transition the density difference and the heat of vaporization both go to zero, when the critical point is approached.

Nevertheless, we have gathered enough information for a realistic construction of the pertinent curves. For nonadecane with a melting point of 305.3 K (= 32.1 °C) we assume that the surface tension for the interface between fluid and vapor (or air) is 30 mN/m at this temperature. To our knowledge this quantity has never been measured, but seems reasonable [13, 14]. The slope of the curve at 20 °C was calculated with the aid of Eq. (27) ρ_g being negligible compared with ρ_l. For ε_{lg} a value of one nanometer was used. In this way one obtains for this slope − 0.142 mN/m K. In Fig. 3 this slope is drawn as a tangent at the said temperature. One also knows that the surface tension and its first derivative with respect to temperature vanish at the critical temperature $T_{cr} = 760$ K. Finally one can also insert the value of the surface tension at the boiling point $T_b = 603$ K, as has been guessed from Eq. (12). The reader may observe that these data furnish together a quite reasonable course of the surface tension of nanodecane as a function of temperature along the co-existence line g–l.

The triple point lies always a little lower than the melting point for "normal" fluids (not for water, of course!). Because of the fact that our situation is quite uncritical in this respect, one is allowed to make a guess for T_3 to be 240 K. At this temperature we jump to the interface tension between liquid and solid by using Eq. (32). Because of $\rho_s - \rho_l \cong 0.1\rho_l$ in almost all cases, σ_{sl} is chosen a factor 10 lower than σ_{lg}. An influence of a possible change in the ε-factors is disregarded in this guess. We shall return to this problem a little later. As a final step in this procedure the sample is (mentally) reheated to the temperature of the melting point. (See again Eq. (27) with properly changed subscripts l → s and g → l.)

Fig. 3 Interface tension of nonadecane against equilibrium temperature along the co-existence lines of the P–T diagram. On the temperature scale one finds from left to right: triple point, melting point, boiling point and critical point. The conclusion, which can be drawn from the surface tension values at T_b and T_m, must be that kinetic barriers for gas–liquid and liquid–solid transition must be of the same order of magnitude

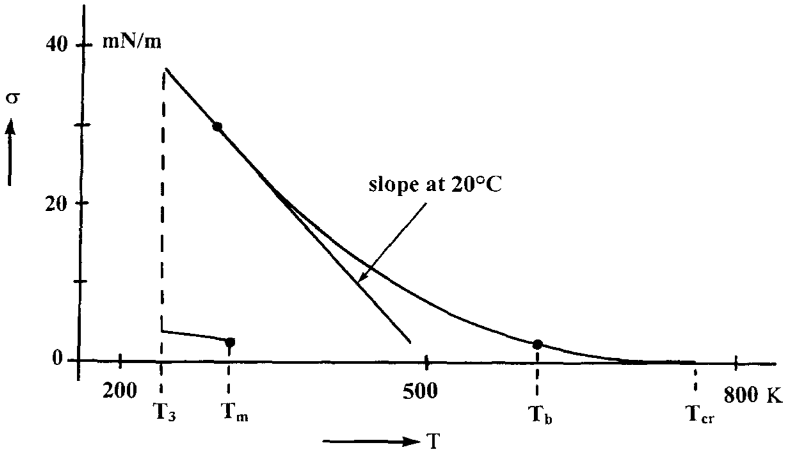

A remark should be added with respect to the fact that crystals possess various crystallographic surfaces. One cannot expect that the respective interface tensions against the fluid are equal. However, the room for variations, as given by Eq. (32), does not seem to be very large. It can only be found in the ε-factors. In fact, the chemical potential μ must be equal on both sides and inside the transitional layer, and also the densities in the homogeneous phases are independent of the considered crystal surfaces. Moreover, one can reasonably assume that the surface layers of the crystal against the fluid are more orderly, in general, than the layer between fluid and gas. The conclusion must be that $\varepsilon_{lg} \geq \varepsilon_{sl}$. So, the ε_{sl}'s can really vary only within a narrow margin.

Undercooling with the crystallization of low molar mass compounds

One can see that with these compounds the order of magnitude of the relevant interface tensions is the same near the boiling and melting points. The conclusion must be that with crystallizing low molar mass compounds the degrees of metastable undercooling cannot be very different from those experienced with the condensation of their vapors. In fact, the relevant interface tensions are rather low. After all, however, this is not too surprising. Even with systems consisting of two practically immiscible fluids like silicon oil and castor oil, which are chemically very different, a value of only 4 mN/m has been reported [15]. A value of only 0.4 mN/m is found for the partially miscible system of butanol and water [13]. For the interface tension between two immiscible polymer melts, viz. those of PS and PMMA, values between 1.8 and 2.2 mN/m were reported by Grammespacher and Meissner [16]. (In heterogeneous polymer blends this interface tension causes a contribution to the storage modulus in the low frequency range.) So for chemically related phases like those of a crystal and its melt one may expect naively a similarly low or even lower average value over the crystal surfaces. As a consequence, one may certainly use Eq. (12) with adequately changed subscripts for a rough (over-) estimate of a possible metastable undercooling.

PART II. POLYMERS

The $T(S)$-diagram for the solidification of i-PP

In Fig. 4 the isobar $T(S)$ is drawn for normal pressure and data of i-PP, as provided by Van Krevelen [14, pp. 112–120]. The data for this poymer were used because of our laboratory experience with this polymer. The (carefully extrapolated) melting point of this polymer lies at a temperature of $T = 208\,^{\circ}\mathrm{C}$ (= 475 K) [17, 18], its entropy of fusion is 18.9 J/mol K. Provisionally it is assumed that the lowest limiting temperature for an effective surface tension barrier ($\geq kT$) lies about 28 degrees below the melting point, viz. at about 180 °C. This lowest level of metastable undercooling is calculated with the assumption of ball-shaped clusters and an interface tension equal to that of nanodecane at its boiling point (see the respective result of Eq. (12), with (nearly) equal values for the "latent" entropies $\Delta H_{tr}/T_{tr}$). This characteristic level of undercooling is indicated in Fig. 4 by a dashed horizontal line. Without any doubt our provisional model, on which this calculation is based, is too primitive for being sufficiently realistic. Surprisingly, however, a more close consideration of the growth mechanisms, as prevailing in polymer melts, will reveal that this estimate is quite useful, nevertheless. In

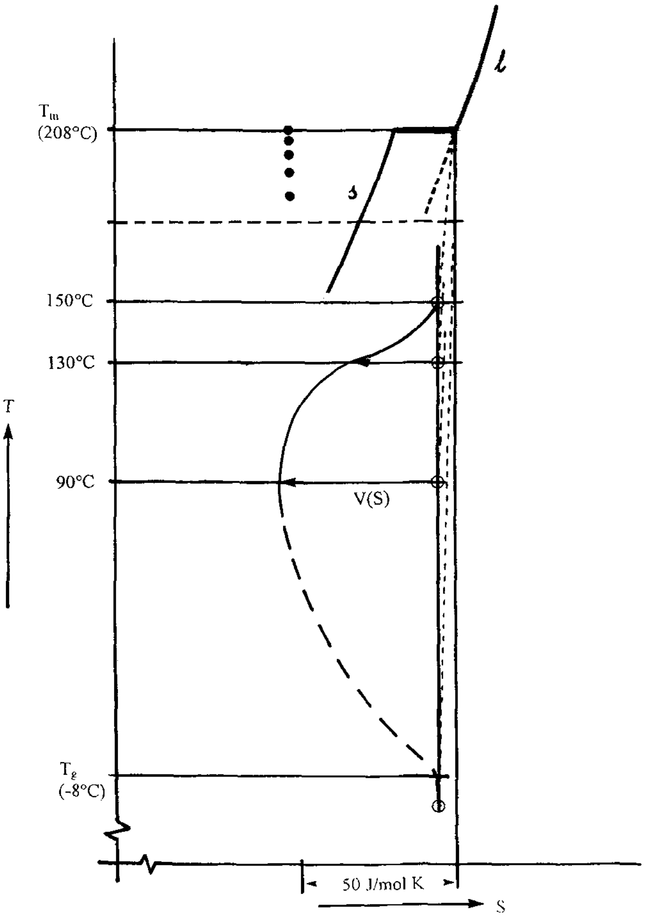

Fig. 4 Isobaric T–S diagram for the liquid–solid transition of i-PP. Overall crystallization speeds $V(S)$ are only schematic. The temperature range for the validity of the classical nucleation theory is indicated by the vertical row of full circles. The lower bound of this range is given by the dashed horizontal line. The "l"-line is extrapolated into the metastable range of undercooling as a dotted line. Several quenches, one of them even below the glass-transition temperature, are indicated by steep dashed lines, clearly ending at points (open circles) characterizing thermodynamically unstable states. Obviously, the crystallization of i-PP occurs entirely in the temperature range of (homogeneous) athermal nucleation

Fig. 4 also an extension of the isobar of the stable fluid into the temperature range below the thermodynamic melting point is inserted as a dotted line. In order to explain the other lines in this figure one has first to describe the concept of a quench adequately. In fact, as is well-known, cooling always occurs at a high rate in all kinds of polymer processing and, also, several important laboratory experiments are deliberately carried out as quenches. As a matter of fact, in highly viscose systems one even finds it impossible to follow the said extended isobar at the desired low pace of cooling. In the given $T(S)$-diagram all more rapid cooling procedures are reflected by lines of steeper slopes than the one observed with the extended isobar. The end-points of these lines clearly characterize non-equilibrium states of the fluid.

In order to understand this statement, one has to consider the second law of thermodynamics a little more closely. A usual formulation of this law is

$$\mathrm{d}q/T \leq \mathrm{d}S \,, \tag{33}$$

where q is the heat irreversibly or reversibly supplied to the system. For the case of cooling, rarely considered in thermodynamics, however, this inequation reads

$$\frac{|\mathrm{d}q|}{T} \geq |\mathrm{d}S| \,. \tag{34}$$

This means that the entropy decreases less with irreversible cooling. The validity of Eq. (34) can also be seen as follows: A cyclic process is constructed, where during heat supply the process is carried out reversibly, whereas during the removal of heat the process is carried out irreversibly, which means that the temperature of the reservoir absorbing the heat is considerably lower than that of the system. According to the well-known integral

$$\oint \frac{\mathrm{d}q}{T} \leq 0 \tag{35}$$

one arrives after this cycle at a value below zero. But this means that more heat is removed from the system than in a completely reversible cyclic process.

A particularly rapid cooling process is a quench of the polymer melt to a temperature below the glass-transition temperature T_g. Such a quench is traced in the figure by an almost vertical (dotted) line. Also three other, somewhat less rapid, quenches are indicated. The temperature scale in this figure is approximately adapted to the situation with i-PP, as mentioned before. We, indeed, succeeded in quenching i-PP to a temperature far below T_g. The advantage of the $T(S)$-plot becomes evident again. One can directly indicate the pertinent temperature changes. The next question is: What happens to the locations of the end-points of the quenches with time? Certainly, these points will travel in horizontal directions, until they meet the $T(S)$-curve for the solid (if the influences of varying morphologies on this curve are disregarded). Without question, the pertinent decrease of entropy will be accompanied by reorganizations in the fluid and by the gradual occurrence of a crystalline phase. One may assume that the progress of overall crystallization will be a useful measure for the speed of internal reorganization. The lengths of the horizontal arrows attached to the end-points of the quenches symbolize the distribution of overall crystallization speeds. The reader may observe that not necessarily a Gaussian distribution should be assumed. There is no doubt that the speed of crystallization is practically zero below the glass-transition temperature and, for i-PP, also above 150 °C. In this connection the reader must be reminded of the findings of Van Krevelen's group [14, 19], according to which the emergence of primary nucleation sites – note the careful formulation (!) – must be particularly conspicuous during the approach of the glass-transition temperature from above. How can it otherwise be that with reheating a tremendous increase of the number of little spherulitical entities is observed? It is also remarkable that, for i-PP, the expected lowest temperature for the existence of a surface tension barrier lies about 25 °C higher than the temperature, where in quiescent melts of i-PP any crystallization activities can be observed within a reasonable time span (see Fig. 4). Below the lower bound of metastable undercooling one is not permitted, in principle, to use the second exponential term of Eq. (1) for the prediction of a sporadic primary nucleation as a function of crystallization temperature.

Present state of the art in polymer crystallization from quiescent melts

For quiescent melts, which are mainly discussed here, the overall rate of crystallization depends on two separate processes: on the appearance of primary nucleation sites and on growth (of lamellae and spherulites). Strictly speaking, one can call the appearance of a nucleation site "primary nucleation" only in the range of metastable undercooling. In fact, nucleation is a process. "Appearance" is considered as something more general in the present context. In our laboratory the measurement of high growth speeds has successfully been developed [9] with the aid of thin layer techniques (see [20]). For the α-modification of i-PP, as defined by Turner-Jones et al. [21], such measurements were possible down to 80 °C. A similar lower temperature limit was reached also for HDPE. For slowly crystallizing polymers this subject is already a classic (see [22, 19]). On the other hand, the problem of the observation of the appearance of primary nucleation sites being, in its generality, a function of time and temperature, is practically unsolved.

Nevertheless, it seems that for many descriptive purposes the assumption of a time independent number of primary nucleation sites $N(T)$ per unit volume, as a unique function of temperature, will suffice [23, 24]. Fortunately, Ziabicki and Alfanso [7] have recently provided theoretical arguments in favor of this simplification. In fact, if with decreasing crystallization temperature sporadic nucleation, as characteristic for the metastable state, ceases to occur, something like a spinodal mode of crystallization should strike the eye, at least, if the pertinent mechanisms are not hampered too much by the low internal mobility. Anyway, the sizes of the required starting areas (proper local arrangements of molecular segments) must be smaller than the smallest sporadically formed nuclei. They probably should be identified with arrangements already formed in the liquid state, which are frozen-in by the quench. However, they do not necessarily become effective all together at the lower border temperature of the metastable undercooling. In this respect the effect of a distribution of their characteristics should be taken into consideration. One may think of sequences of helical conformation forming little aggregates with their likes. (See later in this paper the conditions of lamella growth.) As a consequence, nucleation sites may become effective as "athermal nuclei" in quite a range of (lower) temperatures (see [5]).

In turning to the more practical aspect of the application of those data to structure simulation purposes, one is inclined to become a little polemical. So it has been shown quite recently by Eder [23] and by Eder and Janeschitz-Kriegl [24] with the aid of a formal mathematical proof that the all too well-known so-called isokinetic appraoch [25] is intolerable for the prediction of structures. Our doubts about the usefulness of this approach had already been expressed in earlier papers (see e.g. Eder et al. [26]). It has been invented for a combined and thus simplified isokinetic treatment of primary nucleation and of growth (as caused by secondary nucleation). However, according to the mentioned proof it is unable to describe the influence of the cooling history on structure variations. It just gives the number of spherulites per unit of volume which is predetermined by the a priori assumptions. In this isokinetic approach the temperature range of sporadic nucleation is smeared out in a quite arbitrary way over the whole operative temperature range. Experience shows, however, that the final morphology of a sample depends strongly on the way of cooling: The faster the cooling, the smaller the scale of the single crystalline entities. So, the results of the isokinetic appraoch are in contradiction to reality. This fact seems to be another, indirect support for our angle of view. Interestingly, the simple assumption of a unique temperature function $N(T)$ does not eliminate the possibility for an explanation of the influence of the cooling speed on the final structure of the sample. Admittedly, it makes a distinction between the appearance of athermal homogeneous nucleation sites and heterogeneous nuclei somewhat more difficult. If the latter nucleation is caused by crystalline particles of foreign matter, one can also expect an effect of the cooling speed. In fact, one has to keep in mind that these particles can have various sizes and surface characteristics (different crystal surfaces, edges, holes, etc.), which may become effective at varying temperatures. In general, however, the practical application of heterogeneous nucleation aims at a range of higher temperatures in order to accelerate overall crystallization in an early stage of cooling.

The only direct way of determining numbers of nuclei per unit of volume has been the application of a counting technique. It appears that the thin layer techniques are unreliable because of the uncertainties with respect to the accurate layer thickness ($\cong 5\ \mu$m) and also because of possible influences of the confining cover glasses. With thicker layers, for which the mentioned uncertainties become less important, a sufficiently uniform quench of the sample to the temperature of the coolant becomes difficult. An alternative is given by the application of a steady high cooling rate [27]. In these experiments every volume element of the sample has the same cooling history, on condition that the experiment is started at a sufficiently high temperature and stopped below the temperature of complete crystallization. However, the temperature, at which the crystallization actually happens, remains unknown. A compromise is obtained with DSC-measurements. In these measurements, however, only insufficient cooling rates can be obtained, if one aims at numbers of nuclei at low crystallization temperatures. After the application of a (sometimes serious) correction for internal heat transfer one can use the peak temperature as the temperature of crystallization. In cross-sections of the samples taken from the DSC-pans one can finally carry out the counting. The available temperature range, however, is very restricted with these measurements [28, 29, 24].

In view of this situation one is tempted to propose as a first step a determination of the overall crystallization speed and then a calculation of the number of nuclei with the aid of the measured growth speeds. However, it should be clear to the reader, that an enormous accuracy of both types of measurements would be required. In fact, in the assumed simplifying case of a simultaneous birth of all nuclei the overall degree of crystallinity increases with NG^3, where G is here the growth speed. The required accuracy of G is obvious. For a measurement of the overall crystallization speed the use of Synchrotron radiation (i.e. the use of a high speed X-ray technique) has been recommended (see, e.g. [1, 2]). A very easy estimate of crystallinity is furnished by the measurement of the increasing depolarization of polarized transmittent light. This method is, unfortunately, not completely unambiguous [30]. Light scattering is out of discussion because of its initial sensitivity to NG^6 [9]. In this situation a reliable theory for primary nucleation would be very useful at least as a guide.

The role of the growth mechanism of lamellae for the effectiveness of athermal nucleation sites

The behavior of polymer melts differs in some respects considerably from that of other crystallizable materials. This extraordinary behavior is due to the presence of long chain molecules. From the crystallization in solution one knows that single crystals can be obtained with the shape of platelets in which the chain molecules are in a nearly vertical position with respect to the surface of the platelets. Very often the length of the molecules is much larger than the thickness of the platelets. In these cases the macromolecules are folded back into the lamellar crystals [31, 32]. In the well-known theory of primary sporadic nucleation in solution [33] the formation of rod-like primary nuclei is postulated. By lateral growth on these nuclei the said platelets are formed with a thickness coinciding with the length of the said rod. The rod shape of the primary nucleus is obtained because of the fact that the effective surface tension at the end-surfaces of such a rod is much higher than that at the lateral surfaces, due to the said back-folding. The thickness of such a surface layer, as formed at the end-surface, will become much larger than that of a normal surface layer. So, also a much larger volume of intermediate density will be projected into the interface.

With crystallization from solution the degrees of undercooling are low and the mobility of the chain molecules is high. As a consequence, the metastable situation is fully developed. Clusters of various sizes and shapes are formed and destroyed at almost equal rates. Some of them escape this pseudo-equilibrium by a selection with respect to their size and shape, as provided by the conditions of a passage over the lowest point (a saddle point) of the three-dimensional ridge forming the corresponding barrier. With polymer melts, however, such a situation is almost unthinkable. According to the considerations given above the interface tensions at the "lateral" growth surfaces will not be higher than on the surfaces of the crystals of low molar mass components and, consequently, also not much larger than at the surfaces of growing vapor bubbles with boiling. The corresponding metastable undercooling can be estimated quite easily, as has been shown in this paper. For i-PP this level of undercooling is approximately indicated by the position of the horizontal dashed line in Fig. 4. Below this line one will have for lateral growth:

$$\Delta g_{\mathrm{m,l}} \ll kT\ . \tag{36}$$

As a consequence, this "lateral" growth, which finally must lead to lamellar structures, seems practically unhampered by any barrier of this type. However, it must be realized that this argument can only hold in the beginning of this growth process. In fact, as long as a primary arrangement of molecular segments (in the above described sense) is solitary in a "sea" of the melt, the effective interface tension at the ends of the associated strands can at best be a little larger than on the lateral growth surfaces but will certainly be much smaller than the interface tension at the large side surfaces of a finally resulting lamella. This holds in particular, if this lamella grows in a formation, one lamella near the other, as it happens during spherulite growth. (For the structure of such a surface see below!) In fact, initially, one has a local arrangement of a few chain segments, consisting of helical sequences. Such sequences can snap without much hindrance into the rudiment of a crystal lattice, when the temperature is lowered below the range of metastable cooling, as given by Eq. (36).

Interestingly, even when those rudiments are stable, they can form effective nucleation sites only, if the conditions of further growth are realized. This will be explained in the current paragraph. The necessary helical sequences (of varying length and perfection) must first be formed along single macromolecular chains during a continuous reshuffling of local conformations. This argumentation is infused by the fact that, with macromolecules of a molar mass above a certain critical value, the speed of spherulite growth is found to be independent of the molar mass (see [22]). This fact shows that no gross conformational rearrangements are required as a condition for this growth. In other words, there seems to be no reason for the chain molecules to leave their "tubes" (see [34]) in order to make the way free for suitable new local conformations. In fact, according to these authors an overall reshaping of the molecular coil should require a time proportional to the third power of the molar mass, which would lead to a growth speed inversely proportional to the third power of this molar mass. But this would be in sharp contrast to Magill's findings. If one of the above mentioned helical sequences, travelling along the chain, is locked by association with its equal, mostly stemming from another chain molecule, the local free energy (enthalpy) of this chain will probably decrease a little more than during the preceding spontaneous formation of the sequence. Actually, one can expect some further perfection of the helical conformation and some increase of the length of the sequence, both due to the interaction with the other chain segment. This will certainly cause some extra tensions in the remaining, still tangling parts of the chain molecule. However, one may assume that these tensions will spread along the unattached part of the chain over quite a distance from the locked sequence. This would mean that the extra free energy accumulated at the ends of the locked sequence will remain rather low. This situation, however, will change quickly with increasing lateral dimensions of the lamella (which will have a thickness correspond with the sequence length). One reason for the increase of tensions is the growing restriction in the freedom of tangling. Here some back folding can contribute to a release of tensions. A serious increase of tensions, however, is foreseen for the case that other lamellae start to grow in the near neighbourhood so that the molecular tie strings between the lamellae become shorter, and unavoidable distortions of helices become localized on these strings. (See the origin of the familiar long period in small angle X-ray scattering.) In this way, one will arrive at a rather high and constant level of the excess free energy at the ends of the sequences, when true spherulite growth sets in. This situation was envisaged, when the opening remark of this paragraph was formulated.

If this reasoning is true, no sporadic primary thermal nucleation can occur at temperatures below the temperature calculated from Eq. (12). (For i-PP see the dashed horizontal line at about 180 °C in Fig. 4.) In contrast, tiny crystal rudiments in the above sense, as characterized by a distribution of shapes and sizes will already be present as a consequences of previous thermal histories. Dependent on the individual characteristics of such a rudiment it will become an effective nucleation site only at a temperature, where the corresponding conditions of spherulite growth are fulfilled.

Now it will be clear, why under the conditions of true spherulite growth the barrier for lateral lamellar growth must, in contrast to Eq. (36), obey the following condition:

$$\Delta g_{\mathrm{m.e}} \gg kT \, . \tag{37}$$

Based on these condition Strobl [3, p. 158] quite recently formulated an interesting theory for the growth speed of spherulites. For a realistic crystallization temperature T_{k} (with $T_{\mathrm{k}} < T_{\mathrm{m}}$) one can always find an appropriate lamella thickness, for which this T_{k} represents a pseudo-equilibrium melting point. In fact, the thermodynamic equilibrium melting point T_{m} only holds for an infinite lamella thickness, viz. for completely stretched sequences of monomeric units (zig-zag or helix). If a sequence of a finite number of n^* monomeric units is contained in a lamella (of finite thickness), the extra free enthalpy of the units at the two ends of the sequence (i.e. $2\sigma_{\mathrm{m,e}}$) causes the addressed melting point depression ($T_{\mathrm{m}} - T_{\mathrm{k}}$). At the considered crystallization temperature T_{k} shorter sequences cannot take part in the crystallization process. They cannot be attached permanently to the lamella. In fact, for lamellae built from these sequences the pseudo-equilibrium melting point is below T_{k}. On the other hand, longer sequences with $n > n^*$ can certainly be attached at this temperature to a lamella of suitably larger thickness. For those sequences there is a certain thermodynamic driving force. Their participation in lateral growth is mainly hampered by transport difficulties. The pertinent transport term contains a factor reflecting the probability for a spontaneous outlining of a sequence of n units. This probability Φ decreases with increasing number n of units according to

$$\Phi = (\Phi_0 < 1)^n \approx \exp(-\mu n) , \tag{38}$$

where the factor $\mu > 0$ should not be confused with the chemical potential. This dependence of Φ on n causes a maximum growth speed for sequences of a number of units close to n^*, which corresponds to the chosen crystallization temperature. As a consequence the lamella thickness characteristic for the chosen crystallization temperature T_k dominates in the obtained sample. In this way Strobl arrives at two equations, one for the lamella thickness and one for the growth speed G of the lamellae (not be confused with the free enthalpy G of previous sections). The first equation reads

$$d_c = a_m\left(n^* + \frac{1}{\mu}\right) , \tag{39}$$

with a_m being the length of the monomeric unit. The value of n^* as a function of temperature is not reproduced here. It decreases with decreasing temperature. The second equation reads

$$G \propto \exp\left(-\frac{T_A}{T_k - T_V}\right)\frac{\Delta h_m}{kT_m}\frac{T_m - T_k}{T_k} \times \exp\left(-\frac{2\mu\sigma_{m,e}T_m}{(T_m - T_k)\Delta h_m}\right) . \tag{40}$$

In this latter equation the first factor is the well-known Vogel–Fulcher term (see e.g. [35]) for the description of the influence of transport difficulties, with T_A being an activation temperature ($= E_a/k$), T_V being the Vogel temperature ($\cong T_g - 50$ K). With $T_V = 0$ the Arrhenius term of Eq. (1) is regained. (As Van Krevelen [14, p. 595] has pointed out, close to the melting point the Arrhenius term gives better results.) The second factor of Eq. (40) describes the driving force, as caused by the undercooling, Δh_m being the heat of fusion per mol of monomeric units. The third term becomes equal to one, if the factor μ is zero – no influence of the length of the sequence on the probability of its sporadic formation – an unrealistic proposition. This term contains the extra free enthalpy $\sigma_{m,e}$ for the terminal units of the sequences. Unfortunately, the values of μ and $\sigma_{m,e}$ are unknown. Nevertheless, there are two reasons for satisfaction with this result:

First of all we can now understand why normal growth of spherulites can occur also at large degrees of undercooling, where sporadic primary thermal nucleation is out of question. The extremely high barrier characterized by Eq. (37) is responsible for the occurrence of a quite regular morphology unexpected for a "spinodal" mode of crystallization. Probably, such a regular morphology will disappear, as soon as the third factor of Eq. (40) approaches unity at sufficiently low temperatures.

In the second place one can also be happy from a practical point of view at least, if one is interested in the growth problem as such: the well-known equations for the growth speeds of spherulites as functions of crystallization temperature, as given by Van Krevelen [14, p. 598], are not disqualified by this more rigorous treatment. In fact, the mathematical form of Van Krevelen's equations, which are nominally derived from the theory for secondary nucleation in solution, is similar to that of Eq. (40). Only the second, nonexponential term, representing the thermodynamic driving force for the lamellar growth, is omitted in Van Krevelen's equations. In principle, it must cause a certain obliqueness of the bell-shaped curve of $G(T)$ which, however, may not easily be observable. This second, (linear) nonexponential term or any more accurate term for higher values of $(T_m - T_k)$, will probably become of importance only at undercoolings, where the third term has already approached unity. The good luck of Van Krevelen's equations is that their parameters have been fitted with purely experimental data, as obtained by Magill [22] and Mandelkern et al. [36]. In this respect also one of Van Krevelen's observations is of importance, viz. that most of the experimental data have been obtained with relatively slowly crystallizing polymers with slowly growing spherulites, for which the distance between the temperatures of the melting point and of the glass transition is comparatively small so that a really high degree of undercooling cannot be applied. For fast crystallizing polymers, for which the distance between T_m and T_g can become rather large, no data have ever been obtained for the lower branch of the bell-shaped growth curve $G(T)$, where the growth speed decreases until the glass transition temperature is reached. Interestingly enough, in the high temperature range data for HDPE seem to be in agreement with Van Krevelen's curve, whereas data for i-PP deviate considerably [9]. In this respect, however, the occurrence of other than the most stable crystal modification can considerably disturb the picture.

Final remarks

In the future, also the exploration of the nucleation behavior of moving polymer melts should be continued. The main effects of flow may be: The promotion of disentanglement, the creation of longer sequences of aligned monomeric units in the melt (as a consequence of chain extension) and, last not least, a convective transport mechanism supporting translatory diffusion. These expectations are not in contradiction to the results of our previous work aimed at the unraveling of the processes accompanying the formation of thread-like precursors (as primary nuclei) in i-PP melts at high shear rates [37, 38] see also [39, 40]. From these papers it follows that something like the mechanical work done on the volume element is the decisive parameter. This work is a time integral over the product of shear stress and shear rate. The first factor of this product stands for the chain extension, the second one is a measure for a convective transport mechanism [41].

Some remarks seem appropriate with respect to HDPE. For this polymer the distance of the lower border of metastable undercooling from the melting point is of the same order as with i-PP. But this means that with a melting point of 144 °C, most of the known experiments were carried out in the range of temperatures characteristic for the metastable state. (See, e.g. [42, 43].) So, HDPE forms a special case. Probably, a similar comment may hold also for some other very fast crystallizing polymers. It certainly does not hold for the majority of crystallizing polymers.

A few words should also be said with respect to the "spinodal" modes of crystallization of unoriented PET. For this rather slowly crystallizing polymer all pertinent processes occur in a temperature range corresponding to the lower part of Fig. 4. In this case an interesting parameter is the time span needed for the development of the unisometric pre-stage of a spherulite into a real ball-shaped spherulite. It very much depends on the degree of undercooling, whether one can observe this time span. According to the Japanese authors mentioned it took spherulites of PET about 100 min to approach the ball-shape at 5 °C above the glass-transition temperature. For the temperature range, in which i-PP was investigated so far (down to $T_g + 98$ K), pre-stages can be expected to grow considerably faster and, therefore, cannot be observed easily (see [9]). In fact, according to the WLF-equation (see [34]) the viscosity of a polymer melt decreases by an unbelievable factor 10^{-11} when its temperature is raised from T_g to $T_g + 100$ K! Even if for local motions of parts of the molecule this factor may not be so extreme, the given trend will certainly be correct.

However, the author cannot prevent himself from putting a somewhat contradictory comment at the end of this paper. But the felt necessity for such a step just seems to be characteristic for the unavoidable multifariousness of phenomena in the field of crystallization. Talking about local motions along the polymer chain one may remind oneself of the fact that even in the glassy state such motions are not completely impossible. The possibility for those motions can enhance the toughness of the polymeric glass, as is well-known. Surprisingly, such a local mobility can exist notwithstanding the fact that the overall conformation (coil shape) is immobilized in the glassy state. So, it may also be that a certain reshuffling of sequences can occur in the glass, though on a very modest scale. But this would mean that at higher temperatures, which are still below the border of metastable undercooling, some sporadic appearances of new nucleation sites, as caused by the encounter of two reshuffling trains on neighbouring molecules, cannot completely be excluded. Only, the physical interpretation of such a phenomenon will differ fundamentally from the usual interpretation, as given by Eq. (1). As with the influence on the toughness of glasses, the possibility for such an event will depend very much on the backbone structure of the individual polymer. However, the present author does not believe that the general picture, which he tried to sketch in this paper, will be changed dramatically by this kind of side effects. Only, for some polymers the range of sporadic nucleation will be extended a little bit below the range, calculated for the metastable undercooling. On the other hand, the possibility for an alternative theory of sporadic nucleation can no longer be dismissed.

Conclusions

An estimate for the lower limit for the temperature range in which sporadic nucleation (thermal nucleation) can be expected in quiescent melts of crystallizabe polymers could be given. For this purpose, amongst others, the course of the interface tensions along the co-existence lines of phase diagrams was explored. The conditions, under which athermal nucleation sites emerge at lower temperatures, have been explored as well. In this connection an explanation could be given for the distracting experience that nice spherulites can be found at conditions of severe undercooling where less regular morphologies should be expected.

Acknowledgements The present author wants to express his thanks to Dr. U. Titulaer, Professor of Theoretical Physics at Linz University, for some very valuable discussions and to Dr. M. Cakmak, Professor of Chemical Engineering at the University of Akron, for drawing his attention to this subject. It goes without saying that he acknowledges warmly the continuous possibility for discussions with his colleague Dr. G. Eder, who also gave some important hints for literature quotations.

References

1. Imai M, Kaji K, Kanaya T (1994) Macromolecules 27:7103–8
2. Cakmak M (1996) The 12th Annual Meeting, the Polymer Processing Society, Sorrento, Italy, May 27–31, KN 5.2
3. Strobl G (1996) The Physics of Polymers. Springer Berlin, Heidelberg, New York
4. Becker R (1938) Ann Phys 32:128
5. Zachmann HG (1964) Adv Polym Sci 3:581
6. Becker R, Döring W (1935) Ann Phys 24: 719
7. Ziabicki A, Alfonso GL (1994) Colloid Polym Sci 272:1027
8. Binsbergen FL (1972) J Cryst Growth 16:149
9. Ratajski Ewa, Janeschitz-Kriegl H (1996) Colloid Polymer Sci 274:938
10. Binsbergen FL (1970) Kolloid Z & Zeitschr f Polymere 237:289; 238:389
11. Baehr HD (1996) Thermodynamik, 9th ed (in German) Springer, Berlin, p 185
12. Eder G (1997) Personal communication
13. CRC-Handbook of Chemistry and Physics (1989–90) Weast RC (ed. in chief) 70th ed. CRC Press, Boca Raton, FL
14. Krevelen Van DW (1990) Properties of Polymers. 3rd ed Elsevier, Amsterdam, Oxford, New York, Tokyo
15. Elmendorp JJ (1986) Doctoral thesis, Delft University, The Netherlands
16. Grammespacher H, Meissner J (1992) J Rheol 36:1127
17. Monasse B (1982) Doct Ing Thesis, Ecole Nationale Supèrieure des Mines de Paris
18. Monasse B, Haudin JM (1986) Colloid Polym Sci 264:117
19. Krevelen Van DW (1978) Chimia 32:279
20. Chew S, Griffith JR, Stachurski ZH (1989) Polymer 30:874
21. Turner-Jones A, Aizlewood JM, Backett DR (1964) Makromol Chem 74:134
22. Magill JH, Li HM, Gandica A (1973) J Cryst Growth 19:361
23. Eder G (1996) In: Macromolecular Design in Polymer Materials. Hatada K, Kitayama T, Vogl O (eds) Marcel Dekker, New York, pp 763–784
24. Eder G, Janeschitz-Kriegl H (1997) In: Maijer HEN (ed) Material Science and Technology. Vol 18, Verlag Chemie, Weinheim, pp 269–342
25. Nakamura K, Watanabe T, Katayama K, Amano T (1972) J Appl Polym Sci 16:1077
26. Eder G, Janeschitz-Kriegl H, Liedauer S (1990) Prog Polym Sci 15:629–714
27. Piccarolo S (1992) J Macromol Sci B31:501
28. Janeschitz-Kriegl H, Wippel H, Paulik Ch, Eder G (1993) Colloid Polym Sci 271:1107
29. Wu CH, Eder G, Janeschitz-Kriegl H (1993) Colloid Polym Sci 271:1116
30. Magill JH (1960) Nature 187:770
31. Keller A (1957) Phil Mag 2:1171
32. Geil Ph H (1973) Polymer Single Crystals, RE Krieger Publ Comp, Huntington, NY
33. Lauritzen JI, Hoffman JD (1960) J Res Nat Bur Standards 64A:73
34. Doi M, Edwards SF (1986) The Theory of Polymer Dynamics. Clarendon Press, Oxford
35. Ferry JD (1980) Viscoelastic Properties of Polymers, 3rd ed. John Wiley, New York, Chichester, Brisbane, Toronto, Singapore
36. Mandelkern L, Jain NL, Kim H (1968) J Polym Sci A-2:6, 165
37. Liedauer S, Eder G, Janeschitz-Kriegl H, Jerschow P, Geymayer W, Ingolic E (1993) Int Polym Processing 8:236
38. Liedauer S, Eder G, Janeschitz-Kriegl H (1995) Int Polym Process 10:243
39. Jerschow P, Janeschitz-Kriegl H (1996) Rheol Acta 35:127
40. Jerschow P, Janeschitz-Kriegl H (1997) Int Polym Process 12:72
41. Smoluchowski M von (1917) Z Phys Chemie 92:129
42. Mandelkern L (1964) Crystallization of Polymers, McGraw-Hill, NY
43. Barham PJ, Chivers RA, Keller A, Martinez-Salazar J, Organ SJ (1985) J Material Sci 20:1625
44. VDI-Wärmeatlas (1977) EU Schlünder (ed) 3rd ed, Karlsruhe-Düsseldorf

Note added at proof

Unfortunately, the author only lately recognized a further strong evidence for the correctness of his argumentation. In fact, in a second paper Alfonso and Ziabicki (1995) described characteristic memory effects in very pure samples of i-PP. For the purpose the samples were treated in the following way: first the (very thin samples, embedded between cover glasses) were tempered at 240 °C, a routine well known from the practice of PP-processing. During this treatment nuclei previously formed at lower temperatures are assumed to be destroyed – an interesting fact in itself in view of the argumentation at hand! In a second step the samples were quenched in tap water. In a third treatment the samples were reheated to various "annealing" temperatures (180–260 °C) above the nominal melting point of industrial polypropylenes at 165 °C. At these temperatures the samples were kept for various time spans. Finally, the samples were quenched again to various crystallization temperatures not too far below 165 °C. At these crystallization temperatures the crystallization kinetics were followed by DSC-measurements. This quite elaborate investigation clearly showed that the tendency for crystallization was only eradicated in the course of time at the said "annealing" temperatures. After sufficiently long time, a small crystallization tendency was retained, which was ascribed to times a small amount of permanent heterogeneous nuclei.

Everyone, who has ever followed the melting process of i-PP under the microscope, will agree that close to 165 °C the spherulites disappear. Apparently, however, a lot of nuclei, which do not belong to the type of the heterogeneous nuclei, survives a heat treatment at much higher temperatures for some while! In my opinion this exactly shows that the free energy at the ends of the sequences engaged in Strobl's theory for spherulite growth is not a constant, when the thickness of the associates approaches zero. As a consequence, these associates have a higher "melting point" and remain rather stable at higher temperatures and are able to form the centers for renewed spherulite growth, when the temperature is lowered again.

Reference

Alfonso GL, Ziabicki A (1995) Colloid Polym Sci 273:317